Electrocatalytic Reduction of Carbon Dioxide Based on 2,2'-Bipyridyl Complexes of Osmium

Mitchell R. M. Bruce,† Elise Megehee,‡ B. Patrick Sullivan,*,§ H. Holden Thorp,‖ Terrence R. O'Toole,⊥ Allison Downard,⊛ J. Richard Pugh,# and Thomas J. Meyer*

Department of Chemistry, The University of North Carolina, Chapel Hill, North Carolina 27599-3290

Received February 7, 1992

The complex *cis*-$[Os(bpy)_2(CO)H]^+$ (bpy is 2,2'-bipyridine) has been found to be an electrocatalyst for the reduction of CO_2 in CH_3CN containing 0.1 M tetra-*n*-butylammonium hexafluorophosphate at glassy carbon or Pt electrodes. Under anhydrous conditions CO is the dominant product, but addition of water results in up to 22% formate anion. Kinetic parameters derived by digital simulation of cyclic voltammograms under electrocatalytic conditions are consistent with a rate-determining associative step (k_1) in which CO_2 undergoes a reaction with the direduced complex, $[Os(bpy)_2(CO)H]^-$, to form an intermediate. This intermediate either gives CO or a second intermediate which is a source of CO or formate by competitive pathways that follow the rate-determining step(s). On the basis of the results of isotopic labeling studies, neither the bound CO nor H^- groups are involved in the reduction of CO_2. The kinetics of reduction of CO_2 by the twice-reduced complexes *cis*-$[M(bpy)_2(CO)R]^-$ (M = Os, R = H, Me, Ph; M = Ru, R = CH_2Ph) have also been investigated. From these data, it has been found that a linear correlation exists between ln k_1 and the cone angle of the group, $-R$.

Introduction

A number of group VIII transition metal complexes have been reported to be electrocatalysts for the reduction of carbon dioxide.[1,2] Some information concerning the key redox steps is available,[1-3] but in the main, the detailed mechanistic insight required to design new catalysts that operate at low overvoltages at high rates and with product selectivity remains to be acquired. We report here the results of a kinetic and mechanistic investigation on the reactions between the twice-reduced forms of *cis*-$[Os(bpy)_2(CO)H]^+$ (bpy is 2,2'-bipyridine) and some related complexes with CO_2 in acetonitrile. These results, which appeared in preliminary form as a communication,[4] reveal a, heretofore, unidentified pathway for the reductive activation of carbon dioxide. In this pathway CO_2 adds to the twice-reduced complexes by an associative step apparently involving expansion of the coordination sphere. This gives an intermediate that subsequently forms carbon monoxide or formate anion, the ratio of which depends on the water content of the solution.

Experimental Section

Materials. Salts of the type *cis*- or *trans*-$[M(bpy)_2(CO)R][PF_6]$ (M = Ru, Os) were prepared by procedures described previously.[5] Acetonitrile (Burdick and Jackson) used in the electrochemical experiments was either used as received or distilled over CaH_2 depending on the level of H_2O desired. The supporting electrolyte, tetra-*N*-butylammonium hexafluorophosphate (TBAH), was prepared by metathesis of tetra-*N*-butylammonium bromide and HPF_6 in H_2O. The salt was purified by reprecipitation from CH_2Cl_2/ether and dried in vacuo at 80 °C. Molecular sieves were Linde 4-Å 8 × 12 pellets. The CO_2 gas was anaerobic or bone dry grade (Matheson), and the CO_2/N_2 gas mixtures were certified standard grades (Matheson).

Electrochemical Measurements. Cyclic voltammetric (CV) experiments were conducted by using a Princeton Applied Research 173 potentiostat with a home-built sweep generator and an HP 7015B XY recorder. Solutions for CV measurements in 0.1 M TBAH in CH_3CN (0.5-4.2 mM in metal complex) were made up in a 5-mL volumetric flask. Approximately 3-mL aliquots of the solutions were transferred to a single compartment electrochemical cell with a Teflon top that had provisions for a gas inlet line in addition to the working, auxiliary, and reference electrodes. All solutions were initially purged for a minimum of 10 min with Ar or CO_2/N_2 gas mixtures that were presaturated with CH_3CN (to minimize volume changes). In all experiments a Pt wire auxiliary electrode and a NaCl-saturated calomel reference electrode (SSCE) were employed with either a Pt (0.03 cm^2) or glassy-carbon (0.03 cm^2) working electrode. The $E_{1/2}$ values reported were calculated from $E_{1/2} = {}^1/_2(E_{p^a} + E_{p^c})$ where E_{p^a} and E_{p^c} are the anodic and cathodic peak potentials. The electrodes were polished daily before use with 1-μm diamond polish (Metadi) and were wiped clean prior to each CV measurement. Addition of distilled H_2O (18 MΩ grade) was made by syringe and the solution degassed for several minutes before measurements were made. In general, CV's were recorded from −0.6 to −1.8 V at the sweep rate of interest. Background CV's (i.e., 0.1 M TBAH/CH_3CN)

† Current address: University of Maine, Orono, ME 04412.
‡ Current address: Barnard College, New York, NY 10027.
§ Current address: University of Wyoming, Laramie, WY 82071.
‖ Current address: North Carolina State University, Raleigh, NC 27695.
⊥ Current address: Eastman Kodak Corp., Rochester, NY 14650.
⊛ Current address: University of Canterbury, Christchurch 1, New Zealand.
Current address: National Renewable Energy Laboratory, Golden, CO 80401.

(1) (a) Meshitsuka, S.; Ichikawa, M.; Tamaru, K. *J. Chem. Soc., Chem. Commun.* **1974**, 158. (b) Hiratsuka, K.; Takahashi, K.; Sasaki, H.; Toshima, S. *Chem. Lett.* **1977**, 1137. (c) Takahashi, K.; Hiratsuka, K.; Sasaki, H.; Toshima, S. *Chem. Lett.* **1979**, 305. (d) Eisenberg, R.; Fisher, B. *J. Am. Chem. Soc.* **1980**, *102*, 7363. (e) Tezuka, M.; Yajima, T.; Tsuchiya, A. *J. Am. Chem. Soc.* **1982**, *104*, 6834. (f) Kapusta, S.; Hackerman, N. *J. Electrochem. Soc.* **1984**, *131*, 1511. (g) Becker, J. Y.; Vainas, B.; Egar, R.; Kaufman, L. *J. Chem. Soc., Chem. Commun.* **1984**, 328. (h) Lieber, C. M.; Lewis, N. S. *J. Am. Chem. Soc.* **1984**, *106*, 5033. (i) Beley, M.; Collin, J.-P.; Ruppert, R.; Sauvage, J.-P. *J. Chem. Soc., Chem. Commun.* **1984**, 1315. (j) Wagenknecht, J. H.; Slater, S. *J. Am. Chem. Soc.* **1984**, *106*, 5367. (k) Ishida, H.; Tanaka, K.; Tanaka, T. *Chem. Lett.* **1985**, 405. (l) O'Toole, T. R.; Margerum, L. D.; Westmoreland, T. D.; Vining, W. J.; Murray, R. W.; Meyer, T. J. *J. Chem. Soc., Chem. Commun.* **1985**, 1416. (m) Sullivan, B. P.; Bolinger, C. M.; Conrad, D.; Vining, W. J.; Meyer, T. J. *J. Chem. Soc., Chem. Commun.* **1985**, 1414. (n) Bolinger, C. M.; Sullivan, B. P.; Conrad, D.; Gilbert, J. A.; Story, N.; Meyer, T. J. *J. Chem. Soc., Chem. Commun.* **1985**, 796. (o) Andre, J.-F.; Wrighton, M. S. *Inorg. Chem.* **1986**, *34*, 67. (p) Surridge, N. A.; Meyer, T. J. *Anal. Chem.* **1986**, *58*, 1576. (q) Breikas, A. I.; Abruna, H. D. *J. Electroanal. Chem. Interfacial Electrochem.* **1986**, *201*, 347. (r) Pearce, D. J.; Pletcher, D. *J. Electroanal. Chem. Interfacial Chem.* **1986**, *201*, 317. (s) Kusuda, K.; Ishihara, R.; Yamaguchi, H. *Electrochim. Acta* **1986**, *31*, 657. (t) Hawecker, J.; Lehn, J.-M.; Ziessel, R. *Helv. Chem. Acta* **1986**, *69*, 1990. (u) Sullivan, B. P.; Meyer, T. J. *Organometallics* **1986**, *5*, 1500.

(2) (a) O'Toole, T. R.; Sullivan, B. P.; Bruce, M. R. M.; Margerum, L. D.; Murray, R. W.; Meyer, T. J. *J. Electroanal. Chem. Interfacial Electrochem.* **1989**, *259*, 217. (b) Hurrell, H. C.; Mogstad, A.-L.; Usifer, D. A.; Potts, K. T.; Aburña, H. D. *Inorg. Chem.* **1989**, *28*, 1080. (c) Tanaka, K.; Matsui, T.; Tanaka, T. *J. Am. Chem. Soc.* **1989**, *111*, 3765. (d) Tanaka, K.; Wakita, R.; Tanaka, T. *J. Am. Chem. Soc.* **1989**, *111*, 2428. (e) Sugimura, K.; Kuwabata, S.; Yoneyama, H. *J. Am. Chem. Soc.* **1989**, *111*, 2361. (f) Rasmussen, S. C.; Richter, M. M.; Yi, E.; Place, H.; Brewer, K. J. *Inorg. Chem.* **1990**, *29*, 3926. (g) Schmidt, M. H.; Miskelly, G. M.; Lewis, N. S. *J. Am. Chem. Soc.* **1990**, *112*, 3420. (h) DuBois, D. L.; Miedaner, A.; Haltiwanger, R. C. *J. Am. Chem. Soc.* **1991**, *113*, 8753.

0020-1669/92/1331-4864$03.00/0

were run prior to each set of experiments. All experiments were run at ambient temperatures (20–23 °C).

The diffusion coefficient for *cis*-$[Os(bpy)_2(CO)H][PF_6]$ in CH_3CN was found to be 2.4 (±1.0) × 10^{-6} cm^2/s by CV measurements by employing the Randles–Sevcik equation (eq 1).[6]

$$D = [i_p/(-2.69 \times 10^5)(n^{3/2})(C_0^{\infty})(v^{1/2})]^2 \quad (1)$$

In eq 1, i_p is the peak value of the current amplitude in amperes per cm^2, n is the number of electrons transferred, C_0^{∞} is the bulk concentration of the electroactive species in moles per cm^2, and v is the scan rate in V/s. The peak current was measured at the first reduction wave and n was assumed to equal 1. The results from 30 CV experiments with 4.2 mM *cis*-$[Os(bpy)_2(CO)H][PF_6]$ at scan rates from 0.01 to 0.2 V/s were averaged. The experimentally determined diffusion coefficient was in good agreement with values found elsewhere for related complexes (e.g., D = 4.0 × 10^{-6} cm^2/s for $Ru(typ)(bpy)(OH_2)^{2+}$).[7] The diffusion coefficient of CO_2 in aqueous solution has been estimated to be ~1 × 10^{-5} cm^2/s by Kapusta and Hackerman and 3.05 × 10^{-5} cm^2/s in CH_3CN by Eggins and McNeill.[8]

Constant Potential Electrolysis. A three-compartment cell designed for handling air-sensitive materials as well as sampling the gas above the reaction solution was used for all constant potential electrolysis experiments.[9] The reference electrode was a saturated sodium chloride calomel electrode (SSCE) brought into the main compartment via a lugin capillary. The main compartment contained a cylindrical Pt mesh electrode and a Teflon stir bar centered within the Pt mesh. The auxiliary Pt mesh electrode was separated from the main compartment by a fine glass frit. In order to equalize pressure differences between the main compartment and auxiliary compartments, a small hole was placed above the surface of the solution in the glass wall between the compartments. This allowed the gases to mix but not the solutions. In addition, the cell was connected to an oil bubbler via an 18-gauge stainless steel needle and a short piece of Tygon tubing. These pressure-equalizing features prevented mixing of the solutions in the main and auxiliary compartments as the cell became pressurized, due to the production of CO. The total gas volume of the main and auxiliary compartments was estimated to be 41.5 mL when 25 mL of solution was present in the main and auxiliary compartments. There was some loss of gaseous products from the apparatus during the electrolyses. This led to a systematic error in the analysis for CO that underestimated its production by ≈5–20% in a "typical" experiment, depending somewhat on the duration of the electrolysis. This resulted in material balances that were less than 100%. No attempt was made to account for this error by correcting the results of individual experiments.

In each constant potential electrolysis experiment, the apparatus was assembled, after oven drying, and cooled under an atmosphere of Ar or CO_2. The electrolytic solution was introduced into the cell and degassed with the appropriate gas or gas mixture for a minimum of 10 min with stirring. If molecular sieves were added, they were added just prior to purging. The rotation rate of the magnetic spin bar was kept approximately constant throughout the experiment. The solution was potentiostated at −1.40 V, and after the current had reached a steady state, typically within 5–10 min, the background current (i_{bkg}) was measured. This measurement was used to estimate the water concentration, since the rate of hydrogen evolution at the electrode was shown to be linearly proportional to $[H_2O]$ at −1.40 V under our experimental conditions. In the experiments with added water, a known amount of water was added and the background current was recorded. The catalyst was introduced, the solution purged for an additional 10 min, and the electrolysis initiated at −1.40 V. The steady-state current in the presence of CO_2 (i_{CO_2}) was measured after 10–15 min.

The electrolysis potential of −1.40 V is on the foot of the second reduction wave for the catalyst, but with stirring gave significant catalytic current levels. This potential was chosen to minimize H_2 evolution at the Pt electrode. Similar results were obtained at more negative potentials (to −1.6 V) but there was an increase of 20–30% in the background current. Electrolyses at the first wave with stirring failed to give catalytic currents.

Gas samples were analyzed for CO by means of a Hewlett Packard 5890A gas chromatograph with a 5-Å molecular sieve column attached to the thermal conductivity detection channel by using He as the carrier gas. UV–vis measurements were made in 1-cm quartz cuvettes with Bausch and Lomb Spectronic 2000 or Hewlett–Packard 8451A diode array spectrophotometers. FTIR measurements were made in 0.1-mm-pathlength NaCl solution cells by means of a Nicolet 20 DX spectrophotometer. Analysis of anionic products was carried out with a Dionex 2000i ion chromatograph. TBAH was removed from the reaction solutions prior to analyzing for anionic products by the following procedure: distilled water was added to the reaction solution in a 2:1 ratio (H_2O/total reaction volume), and the resulting solution was concentrated and filtered through Q5 (Fisher) filter paper to remove TBAH (the solubility of TBAH in H_2O is <5 × 10^{-4} M). Control experiments with standard solutions in which Cl^-, Br^-, oxalate, glyoxylate, glycolate, and formate were added as anions gave an average recovery from the column of 92% ± 8% by using this procedure. There was no interference by PF_6^-.

Computer Simulation of Cyclic Voltammograms. The method of finite differences[10] was used to predict how the ratio of the diffusion to catalytic peak currents at the second reduction wave was affected by different experimental conditions for several mechanisms. The algorithm for two, sequential, redox couples was taken from a paper by Feldberg.[10e] Our procedure consisted of the following steps: (1) A particular mechanism was assumed, and the differential form of the mechanism and the appropriate boundary conditions were transcribed into the finite difference form. (2) The program incorporating the results of step 1 was run for a range of rate constants. (3) The predicted and experimental results were compared. The differential equations used for a catalytic cycle consisting of electron transfer (reactions 9 and 10, see Results and Discussion), water independent reduction of CO_2 (reactions 14 and 15), and the reduction of CO_2 with water involvement (reactions 18 and 20) are given in eqs 2–8. In these equations Os = *cis*-$[Os(bpy)_2(CO)H]^+$, t = time, x = distance from the electrode, and D is the diffusion coefficient, which was assumed to be the same for the various species, D = 2.6 × 10^{-6} cm^2/s. The symbols I_a and I_b are for intermediates that appear in the reaction. The mechanism is presented in detail in the Results and Discussion. Equations 2–8 show the time dependence of each of the

(3) (a) Sullivan, B. P.; Bruce, M. R. M.; O'Toole, T. R.; Bolinger, C. M.; Megehee, E.; Thorp, H.; Meyer, T. J. *Adv. Chem. Ser.* **1988**, *363*, 52 and references therein. (b) Behr, A. *Carbon Dioxide Activation by Metal Complexes*; VCH: Weinheim, Germany, 1988; see also references therein. (c) Maher, J. M.; Cooper, N. J. *J. Am. Chem. Soc.* **1980**, *102*, 7604. (d) Keene, F. R.; Creutz, C.; Sutin, N. *Coord. Chem. Rev.* **1985**, *64*, 247. (e) Darensbourg, D. J.; Kudarowski, R. *J. Am. Chem. Soc.* **1984**, *106*, 3672. (f) Darensbourg, D. J.; Hanckel, R. K.; Bauch, C. G.; Pala, M.; Simmons, D.; White, J. N. *J. Am. Chem. Soc.* **1985**, *107*, 7463. (g) Sullivan, B. P.; Meyer, T. J. *Organometallics* **1986**, *5*, 1500. (h) Fujita, E.; Szalda, D. J.; Creutz, C.; Sutin, N. *J. Am. Chem. Soc.* **1988**, *110*, 4870. (i) Sakaki, S.; Ohkubo, K. *Organometallics* **1989**, *8*, 2970. (j) Tsai, J.; Khan, M.; Nicholas, K. M. *Organometallics* **1989**, *8*, 2967. (k) Eisenschmid, T. C.; Eisenberg, R. *Organometallics* **1989**, *8*, 1822. (l) Alvarez, R.; Carmona, E.; Galindo, A.; Gutiérrez, E.; Marin, J.; Monge, A.; Poveda, M. L.; Ruiz, C.; Savariault, J. M. *Organometallics* **1989**, *8*, 2430. (m) Sakaki, S.; Ohkubo, K. *Inorg. Chem.* **1989**, *28*, 2583. (n) Silavwe, N. D.; Goldman, A. S.; Ritter, R.; Tyler, D. R. *Inorg. Chem.* **1989**, *28*, 1231. (o) Bo, C.; Dedieu, A. *Inorg. Chem.* **1989**, *28*, 304. (p) Sakaki, S. *J. Am. Chem. Soc.* **1990**, *112*, 7813. (q) Lundquist, E. G.; Huffman, J. C.; Folting, K.; Mann, B. E.; Caulton, K. G. *Inorg. Chem.* **1990**, *29*, 128. (r) Amatore, C.; Jutand, A. *J. Am. Chem. Soc.* **1991**, *113*, 2819. (s) Vites, J. C.; Steffey, B. D.; Giuseppetti-Dery, M. E.; Culter, A. R. *Organometallics* **1991**, *10*, 2827. (t) Alvarez, R. A.; Atwood, J. L.; Carmona, E.; Pérez, P. J.; Poveda, M. L.; Rogers, R. D. *Inorg. Chem.* **1991**, *30*, 1493. (u) Darensbourg, D. J.; Mueller, B. L.; Bischoff, C. J.; Chojnacki, S. S.; Reibenspies, J. H. *Inorg. Chem.* **1991**, *30*, 2418. (v) Creutz, C.; Schwarz, H. A.; Wishart, J. F.; Fujita, E.; Sutin, N. *J. Am. Chem. Soc.* **1991**, *113*, 3361. (w) Sakaki, S. *J. Am. Chem. Soc.* **1992**, *114*, 2055. (x) Tanaka, H.; Nagao, H.; Peng, S.; Tanaka, K. *Inorg. Chem.* **1992**, *31*, 1450.

(4) Bruce, M. R. M.; Megehee, E.; Sullivan, B. P.; Thorp, H.; O'Toole, T. R.; Downard, A.; Meyer, T. J. *Organometallics* **1988**, *7*, 238.

(5) (a) Sullivan, B. P.; Casper, J. V.; Johnson, S. R.; Meyer, T. J. *Organometallics* **1984**, *3*, 1241. (b) Megehee, E. Ph.D. Thesis, The University of North Carolina, Chapel Hill, NC, 1985.

(6) Greef, R.; Peat, R.; Peter, L. M.; Pletcher, D.; Robinson, J. *Instrumental Methods in Electrochemistry*; Halsted Press and John Wiley And Sons: New York, 1985; Chapter 6.

(7) McHatton, R. C.; Anson, F. C. *Inorg. Chem.* **1984**, *23*, 3935.

(8) (a) Kapusta, S.; Hackerman, N. *J. Electrochem. Soc.* **1984**, *131*, 1511. (b) Eggins, B. R.; McNeill, J. *J. Electroanal. Chem.* **1983**, *148*, 17.

(9) Bolinger, C. M.; Story, N.; Sullivan, B. P.; Meyer, T. J. *Inorg. Chem.* **1988**, *27*, 4582.

(10) (a) Feldberg, S. W. In *Electroanalytical Chemistry*; Bard, A. J., Ed.; Marcel Dekker: New York, 1969; Vol. 3. (b) Feldberg, S. W. In *Computer Applications in Analytical Chemistry*; Mark, H. B., Ed.; Marcel Dekker: New York, 1972; Vol. 2, Chapter 7. (c) Zizelman, P. M.; Amatore, C.; Kochi, J. *J. Am. Chem. Soc.* **1984**, *106*, 3771. (d) Feldberg, S. W. *J. Phys. Chem.* **1971**, *75*, 2377. (e) Feldberg, S. W. *Comput. Chem. Instrum.* **1972**, *2*, 185. (f) Bard, A. J.; Faulkner, L. R. *Electrochemical Methods*, John Wiley: New York, 1980. (g) Rieger, P. H. *Electrochemistry*; Prentice-Hall: Englewood Cliffs, NJ, 1987.

$$\partial[Os^+]/\partial t = D(Os^+)(\partial^2[Os^+]/\partial x^2) + k_6[I_b] \quad (2)$$

$$\partial[Os^0]/\partial t = D(Os^0)(\partial^2[Os^0]/\partial x^2) + 2k_2[I_a]^2 \quad (3)$$

$$\partial[Os^-]/\partial t = D(Os^-)(\partial^2[Os^-]/\partial x^2) - k_1[Os^-][CO_2] \quad (4)$$

$$\partial[CO_2]/\partial t = D(CO_2)(\partial^2[CO_2]/\partial x) - k_1[Os^-][CO_2] \quad (5)$$

$$\partial[I_a]/\partial t = D(I_a)(\partial^2[I_a]/\partial x^2) + k_1[Os^-][CO_2] - 2k_2[I_a]^2 - k_5[I_a][H_2O] \quad (6)$$

$$\partial[H_2O]/\partial t = D(H_2O)(\partial^2[H_2O]/\partial x^2) - k_5[I_a][H_2O] \quad (7)$$

$$\partial[I_b]/\partial t = D(I_b)(\partial^2[I_b]/\partial x^2) + k_5[I_a][H_2O] - k_6[I_b][Os^0] \quad (8)$$

components in the diffusion layer owing to diffusion (the first term) and chemical reactions. A general, closed form solution to these equations is not possible. Approximate solutions can be found by transforming the equations into the finite difference form. This involves dividing the diffusion layer into a finite number of volume and time elements in order to estimate the concentration gradients within the diffusion layer by using computer methods. The procedures used for incorporating the differential equations into the computer simulation program can be found in ref 10.

Results and Discussions

The syntheses and spectral properties of *cis*-$[Os(bpy)_2(CO)H][PF_6]$ and the PF_6^- salts of the related complexes of Os^{II} and Ru^{II} studied here have been reported elsewhere.[5] In Figure 1A is shown a CV of a solution containing *cis*-$[Os(bpy)_2(CO)H][PF_6]$ at a Pt working electrode in a 0.1 M TBAH in CH_3CN solution deoxygenated with argon. In a reductive scan to −1.8 V, two reversible, one-electron waves appear corresponding to successive bipyridine-based reductions with $E_{1/2}$ values of −1.34 and −1.59 V vs SSCE, respectively. In oxidative scans, an irreversible one-electron wave is observed at +0.9 V vs SSCE corresponding to the osmium(III/II) couple. When carbon dioxide ($[CO_2]_{sat} \approx 0.14$ M)[11] was introduced into a dry solution ($[H_2O] \sim 3 \times 10^{-3}$ M) the integrated current for the first reduction remained unchanged while the current for the second reduction was greatly enhanced (Figure 1B).[13] From this observation it can be inferred that the doubly-reduced form, *cis*-$[Os(bpy)_3(CO)H]^-$, is reactive toward CO_2 and that the rate law for the reaction includes both the reduced complex and CO_2.

Cyclic Voltammograms in the Presence of H_2O and CO_2. In the absence of complex there was little background current out to −1.8 V at a Pt electrode (0.03 cm^2) in deoxygenated, dry 0.1 M TBAH in CH_3CN. Upon addition of H_2O, a current is produced due to the reduction of H_2O to hydrogen. The onset of this reaction occurs at ≈−1.0 V. This reaction was clearly observable, on a 10 μA/cm X-Y recorder scale, at voltages past −1.6 V when 10 μL of water was added to 4.5 mL of the CH_3CN solution to give a solution ≈0.1 M in H_2O. The current increased in proportion to the amount of water added. Upon the addition of 50 μL of water, a current of about 20 μA was reached at −1.6 V. At glassy-carbon electrodes (0.03 cm^2) the background current was negligible even at concentrations of added H_2O approaching 1.0 M.

In the presence of *cis*-$[Os(bpy)_2(CO)H][PF_6]$ with added water, the only change in the voltammogram in Figure 1A was an increase in the background current due to the hydrogen evolution reaction. Thus, when 50 μL of water was added to a solution 4.2 mM in *cis*-$[Os(bpy)_2(CO)H][PF_6]$ under Ar, a current enhancement of ~20 μA was observed at −1.6 V. We conclude from these observations that the reduced osmium complex does not undergo reactions with water or hydrogen on the time scale of the CV experiment. When the CV experiment was repeated but with added CO_2, the addition of water produced a current level above that due to the background evolution of H_2 (Figure 2). The magnitude of the current enhancement was the same within experimental error at either Pt or glass-carbon electrodes. From this observation it can be inferred that the enhanced current arises from a reaction between doubly reduced *cis*-$[Os(bpy)_2(CO)H]^-$ and H_2O *after* the reduced complex had undergone a reaction with CO_2. Qualitatively, the increase in current as the concentration of CO_2 was increased was far greater than when $[H_2O]$ was increased.

Constant Potential Electrolyses. In the presence of CO_2 at a Pt electrode, solutions 1–2.5 mM in *cis*-$[Os(bpy)_2(CO)H][PF_6]$ show sustained catalytic currents at −1.4 V. Summaries of the results obtained from a series of electrolysis experiments are

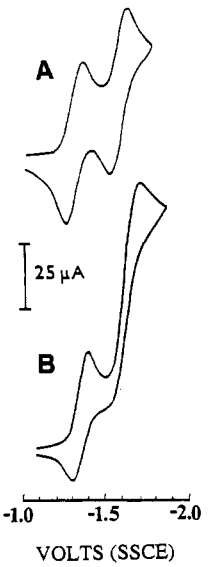

Figure 1. Cyclic voltammograms in MeCN solutions containing 0.1 M TBAH of *cis*-$[Os(bpy)_2(CO)H][PF_6]$ (4.2 mM) at a Pt-button electrode (0.03 cm^2) at a scan rate of 100 mV s^{-1}: (A) argon-bubbled solutions; (B) CO_2-bubbled solutions ($[CO_2] \approx 0.14$ M).

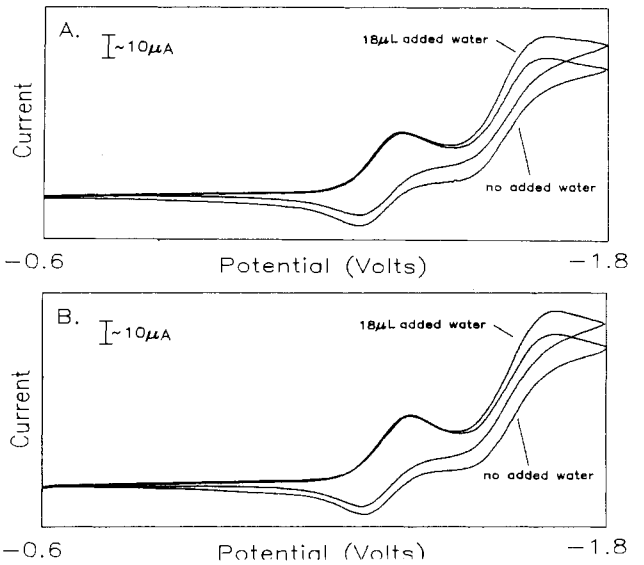

Figure 2. Cyclic voltammograms in MeCN solutions containing 0.1 M TBAH at scan rates of 200 mV s^{-1} with added water as indicated: (A) a solution saturated in CO_2 containing *cis*-$[Os(bpy)_2(CO)H][PF_6]$ (3.9 mM) at a Pt electrode: (B) a solution as in part A but at a glassy-carbon electrode. The original CV's were digitized by using un-Plot-It (Silk Scientific) and plotted from Spectra Calc (Galactic Industries).

(11) The concentration of CO_2 in 0.1 M TBAH/CH_3CN is 0.14 M as measured by GC under similar experimental conditions (see ref 12).
(12) Pugh, J. R.; Bruce, M. R. M.; Sullivan, B. P.; Meyer, T. J. *Inorg. Chem.* **1991**, *30*, 86.
(13) The term dry is used to refer to solutions of CH_3CN in which $[H_2O]$ was typically ~3 × 10^{-3} M.

Table I. Products of Constant Potential Electrolyses at −1.4 in V 0.1 M TBAH in MeCN[a]

expt	complex (1–2.5 mM)	current (mA)		C_{total} (C)	charge used for product (C)[d]		Coulomb balance[e]
		i_{bkg}[b]	i_{CO_2}[c]		C_{CO}	$C_{formate}$	
1	*cis*-$[Os(bpy)_2(CO)H]^+$	4.7	50	82	>40	8.6	>68
2	*cis*-$[Os(bpy)_2(CO)H]^+$	3.3	102	121	>57	3.6	>50
3	*cis*-$[Os(bpy)_2(CO)D]^+$	2.3	15	40	18	7.9	86
4[f]	*cis*-$[Os(bpy)_2(CO)H]^+$	1.3	33	40	30	2.1	86
5	*cis*-$[Os(bpy)_2(CO)H]^+$	16	62	40	14	3.7	79
6	*cis*-$[Os(bpy)_2(CO)H]^+$	2.2	25	40	32	5.1	102
7[g]	*cis*-$[Os(bpy)_2(CO)H]^+$, $^{13}CO_2$	0.25	30	102			
8[g]	*cis*-$[Os(bpy)_2(CO)H]^+$	0.5	45	100			
9[g]	*cis*-$[Os(bpy)_2(CO)H]^+$, $^{13}CO_2$	1.1	30	100	62		66
10[h]	*cis*-$[Os(bpy)_2(CO)H]^+$, $^{13}CO_2$		12	52	28		54
11[i]	*cis*-$[Os(bpy)_2(CO)H]^+$, D_2O	6.3	38	100			

[a] In CO_2-purged solution unless otherwise noted. [b] Steady-state current in the absence of osmium complex reached after approximately 5 min. These currents were used in conjunction with a calibration curve to estimate $[H_2O]$ in the solutions with the results shown in Figure 3. [c] Steady-state current in the presence of CO_2 reached after approximately 10 min. [d] Calculated by including the stoichiometric factor 2 in the reduction of CO_2 to these products. [e] Coulomb balance, expressed as a percentage, is defined as the total Coulombs of products produced, including the background process, divided by the total Coulombs consumed during the experiment: $((C_{CO} + C_{formate} + C_{bkg})/(C_{total})) \times 100$. [f] In this experiment, a cationic membrane was used to separate the working and auxiliary compartments. [g] Carbon dioxide was charged into a ballast vessel (130 mL) connected in series to a peristaltic pump and the electrochemical cell. The cell gases (CO_2 and argon) were recirculated continously by the pump prior to and during the experiment. [h] $^{13}CO_2$ was slowly bubbled into CH_3CN (≈3 mL/min) for 12 min prior to the start of the experiment. The solution was potentiostated at −1.5 V. [i] About 325 μL of D_2O was added to 26 mL of solution (≈0.7 M). The solution was potentiostated at −1.6 V.

Table II. Products of Constant Potential Electrolyses as in Table I Except That the Experiments were Performed over Molecular Sieves

expt	complex (1–2.5 mM)	current (mA)		C_{total} (C)	charge used for product (C)			Coulomb balance[b]
		i_{bkg}	i_{CO_2}		C_{CO}	$C_{formate}$	C_{Ox}[a]	
12	*cis*-$[Os(bpy)_2(CO)H]^+$	0.15	9.0	40	21	6.7	0.0	71
13	*cis*-$[Os(bpy)_2(CO)H]^+$	0.23	9.7	40	22	8.7	0.0	80
14	*cis*-$[Os(bpy)_2(CO)(MeCN)]^{2+}$	0.39	9.7[c]	25	9.7	0.28	0.9	48
15[d]	*cis*-$[Os(bpy)_2(MeCN)_2]^{2+}$	0.37	1.6	10	0.8	0.08	0.26	32
16	*cis*-$[Os(bpy)_2(CO)H]^+$	0.03	4.4[e]	29	18	1.0	0.02	66
17	*cis*-$[Os(bpy)_2(CO)H]^+$	0.39	11.5	40	31	5.3	0.16	94

[a] Coulombs as oxalate anion. [b] As in Table I but defined as $((C_{CO} + C_{formate} + C_{Ox} + C_{bkg})/(C_{total})) \times 100$. [c] The average value. The current decreased during the experiment. The current (i_{CO_2}) at the end of the experiment was 5 mA. [d] The potential was adjusted to −1.45 V midway through the experiment. [e] The average value. The current decreased during the experiment and was accompanied by precipitation. The current (i_{CO_2}) at the end of the experiment was 2.5 mA.

presented in Tables I and II. Both current levels and product yields are cited where the data are available.[14] After 10, two-electron turnovers of *cis*-$[Os(bpy)_2(CO)H]^+$, only a small amount of decomposition of the catalyst had occurred; ~5% by UV–vis and FTIR analysis.[15] Although the point was not pursued in further detail, two plausible decomposition products are *cis*-$[Os(bpy)_2(CO)(CH_3CN)]^{2+}$ and *cis*-$[Os(bpy)_2(CH_3CN)_2]^{2+}$. Although *cis*-$[Os(bpy)_2(CO)(CH_3CN)]^{2+}$ is a catalyst toward CO_2 reduction, it is slow (Table II, experiment 14), while *cis*-$[Os(bpy)_2(CH_3CN)_2]^{2+}$ is relatively inactive (Table II, experiment 15).

The water concentration was estimated from the background steady-state current at −1.4 V prior to the addition of the osmium complex by using a predetermined calibration curve. Constant potential electrolysis of solutions containing *cis*-$[Os(bpy)_2(CO)H][PF_6]$ at low concentrations of water, result in CO as the major product (Faradaic efficiency is high as 80%) with formate appearing as a minor product (3–12%).[16] When water was deliberately added, formate anion increased as a product up to 22%, and carbon monoxide was reduced to levels as low as 46%. In Figure 3 is shown a plot of the electrolysis current that led to formate anion plotted vs the water concentration estimated from the background currents (i_{bkg}) by using a calibration curve. The current that led to formate anion was calculated by the expression

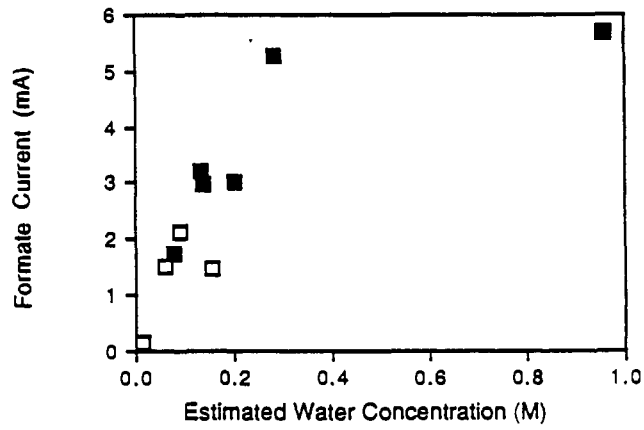

Figure 3. Plot of the estimated catalytic current arising from formate anion production vs the concentration of added H_2O. Data from Table I (■) and Table II (□).

$i_{CO_2}(C_{formate}/C_{total})$. In this expression i_{CO_2} is the catalytic current, $C_{formate}$ the concentration of formate anion produced, and C_{total} the total concentration of reduced CO_2 equivalents (as CO and HCO_2^-). The dependence on $[H_2O]$ appeared to level off at $[H_2O] > 0.4$ M. A series of experiments was also performed in the presence of molecular sieves which were added to lower the concentration of water present in the electrolysis solutions. Similar results were obtained (Table II) and those which relate to formate anion production are included in Figure 3.[17]

Kinetics: No Added Water. The results of a series of electrochemical kinetics studies are listed in Table III. The data,

(14) The product yields are presented as electron equivalents (Coulombs) in the tables. Not all analyses were performed in each experiment. The potential was held at −1.4 V to minimize hydrogen evolution at Pt but still allow catalysis to occur.

(15) The electrolyses typically took 60 min to complete. Limitations in the cell design which led to loss of gaseous products and mixing of solution in the separate compartments prevented substantially longer electrolysis times.

(16) The Faradaic efficiency is defined as follows: [(moles of product)(2 e⁻ per product)/moles of electrons passed] × 100.

(17) The addition of molecular sieves resulted in a change in the slope of the calibration curve of i_{bkg} vs $[H_2O]$. This is likely due to the basicity of the 4-Å molecular sieves; see for example: Breck, D. W. *J. Chem. Educ.* **1964**, *48*, 678, and Figure E.2 in ref 10f.

Table III. Kinetic Parameters for the Electrocatalyzed Reduction of CO_2 by *cis*-$[Os^{II}(bpy)_2(CO)H]^+$ without Added H_2O[a]

expt	concn (mM) $[Os^{II}]$	concn (mM) $[CO_2]$[b]	scan rate v[c]	i_d/i_{CO_2}[d]
1	4.2	140	200	0.63
2	4.2	140	100	0.54
3	4.2	140	50	0.45
4	4.2	140	20	0.38
5	4.2	45	200	0.92
6	4.2	45	100	0.82
7	4.2	45	50	0.71
8	4.2	45	20	0.59
9	4.2	14	200	0.99
10	4.2	14	100	0.96
11	4.2	14	50	0.88
12	4.2	14	20	0.74
13	4.2	1.4	50	1.02
14	4.2	1.4	20	1.00
15	2.1	140	200	0.74
16	2.1	140	100	0.61
17	2.1	140	50	0.54
18	2.1	45	200	0.83
19	2.1	45	100	0.73
20	2.1	45	50	0.64
21	2.1	14	200	0.98
22	2.1	14	100	0.86
23	2.1	14	50	0.84
24	1.0	140	500	0.81
25	1.0	140	200	0.66
26	1.0	140	100	0.61
27	1.0	140	50	0.56
28	1.0	45	500	0.97
29	1.0	45	200	0.90
30	1.0	14	500	0.94
31	1.0	14	200	0.87
32	0.52	140	200	0.67
33	0.52	45	200	0.89

[a] By cyclic voltammetry at a Pt electrode in 0.1 M TBAH in MeCN solution. [b] The concentration of CO_2 was 0.14 M.[21] Ideal gas and Henry's law behaviors were assumed for gas mixtures. [c] Scan rate in mV/s. [d] The ratio of the peak diffusion current in the absence (i_d) and presence (i_{CO_2}) of CO_2 for the second reduction wave of *cis*-$[Os(bpy)_2(CO)H]^+$.

which were acquired in dry CH_3CN [$(H_2O) \sim 3 \times 10^{-3}$ M], are reported as the ratio of peak currents for the second reduction wave of *cis*-$[Os(bpy)_2(CO)H]^+$ in the absence (i_d) and presence of CO_2 (i_{CO_2}) as a function of scan rate, $[CO_2]$, and concentration of catalyst. The variations in peak current were analyzed by the method of finite differences of Feldberg.[10] It has been applied to the determination of rate constants for other reactions.[18]

As a starting point in the analysis we chose to simulate the kinetics of three mechanisms in all of which *cis*-$[Os(bpy)_2(CO)H]^+$ was reduced to *cis*-$[Os(bpy)_2(CO)H]^-$ (eqs 9 and 10) by two sequential, one-electron reductions followed by (1) a rate-determining step (RDS) first order in both CO_2 and twice reduced complex (eq 11), (2) a RDS second order in CO_2 and first order in reduced complex (eq 12), or (3) a RDS first order in CO_2 and second order in reduced complex (eq 13). In all three cases, it was assumed that the RDS was followed by a series of unspecified steps which led to CO and the neutral complex. Equations 11–13 are kinetic equations written without regard to charge, mass, or redox balance. Possible reactions that occur following the RDS are presented below, in eqs 14–17.

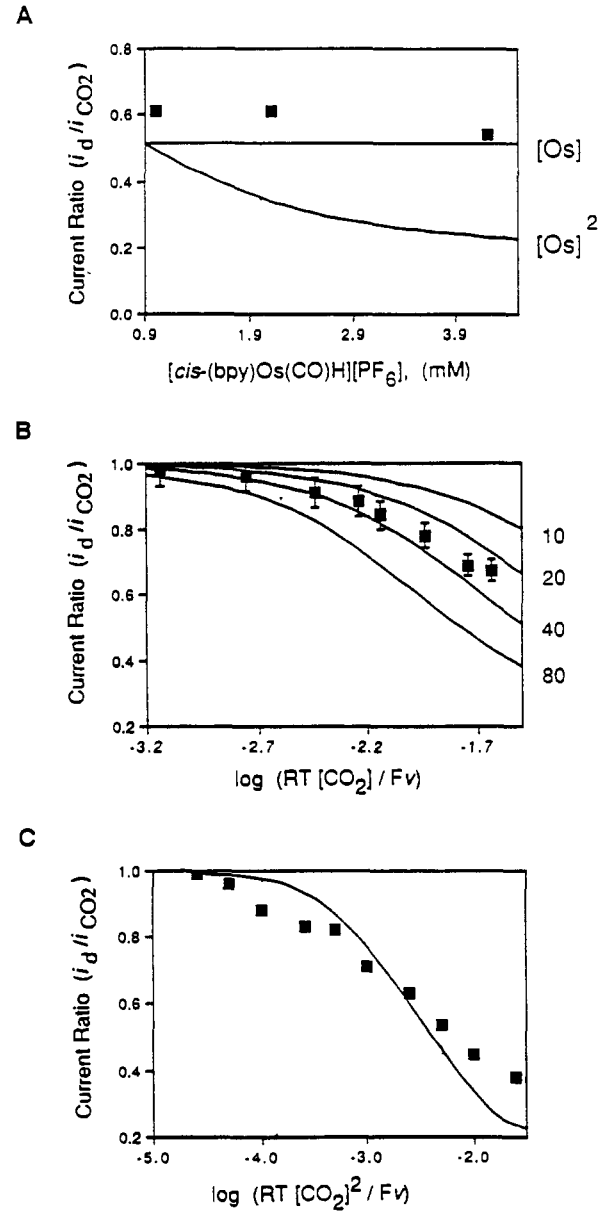

Figure 4. Comparison of CV simulations with the experimental results taken from the data in Table III. (A) i_d/i_{CO_2} vs *cis*-$[Os(bpy)_2(CO)H][PF_6]$ (mM). For the plot vs [Os], the mechanism was assumed to be eqs 9, 10, and 11. The quantities $k_{rds} = 30$ M^{-1} s^{-1}, $[CO_2] = 140$ mM, and scan rate = 100 mV/s were used in generating the working curve. For the plot vs $[Os]^2$, eqs 9, 10, and 13 were assumed with, $k_{rds} = 2.5 \times 10^4$ M^{-2} s^{-1}, $[CO_2] = 140$ mM, and scan rate = 100 mV/s. (B) i_d/i_{CO_2} vs log $(RT[CO_2]/Fv)$ where R = gas constant, T = temperature, F = Faraday's constant, and v = scan rate. The data shown are average values obtained from two to five CV experiments. The simulations were based on eqs 9, 10, and 11 with k_{rds} as indicated with *cis*-$[Os(bpy)_2(CO)H][PF_6]$ at 4.7 mM. Error bars of 5% are shown for the data points. (C) i_d/i_{CO_2} vs log $(RT[CO_2]^2/Fv)$ for a mechanism based on eqs 9, 10, and 12 with $k_{rds} = 350$, and *cis*-$[Os(bpy)_2(CO)H][PF_6]$ at 4.7 mM.

The dependence of the peak current ratio (i_d/i_{CO_2}) on scan rate and the concentrations of complex and CO_2 are sensitive to the mechanistic assumptions made.[19] In Figure 4 are compared experimental points (solid boxes), obtained from the CV experiments, and the results of CV simulations (solid lines). In Figure 4A are shown plots of the ratio, i_d/i_{CO_2}, as a function of the complex concentration. The CV simulations are shown for mechanisms involving eqs 9 and 10 followed by eq 11 or followed by eq 12. In parts B and C of Figure 4 are shown plots of i_d/i_{CO_2}

(18) Zizelman, P. M.; Amatore, C.; Kochi, J. K. *J. Am. Chem. Soc.* **1984**, *106*, 3771.

(19) In applying the finite difference method, the experimentally important parameter is i_d/i_{CO_2}, the ratio of the diffusion current at the peak of the second reduction wave (i_d) to the peak catalytic current in the presence of added CO_2 (i_{CO_2}). The quantity i_{CO_2} was taken to be the difference between the maximum current and an extrapolated baseline. Direct measurement of i_d during the same CV experiment was not possible. The CV experiments were conducted in sets such that the same Os^{II} solution was used while the CO_2 concentration was varied. Within each set a small change in concentration occurred. The quantity i_d was estimated for each experiment by utilizing i_d when $[CO_2] = 0$ and multiplying it by the ratio of peak currents for the first reduction in the presence and absence of CO_2.

$$cis\text{-}[Os(bpy)_2(CO)H]^+ \underset{-e^-}{\overset{+e^-}{\rightleftarrows}} cis\text{-}[Os(bpy)_2(CO)H]^0 \quad (9)$$

$$cis\text{-}[Os(bpy)_2(CO)H]^0 \underset{-e^-}{\overset{+e^-}{\rightleftarrows}} cis\text{-}[Os(bpy)_2(CO)H]^- \quad (10)$$

$$cis\text{-}[Os(bpy)_2(CO)H]^- + CO_2 \overset{k_{RDS}}{\rightarrow} \rightarrow cis\text{-}[Os(bpy)_2(CO)H]^0 + CO \quad (11)$$

$$cis\text{-}[Os(bpy)_2(CO)H]^- + 2CO_2 \overset{k_{RDS}}{\rightarrow} \rightarrow cis\text{-}[Os(bpy)_2(CO)H]^0 + CO \quad (12)$$

$$2\ cis\text{-}[Os(bpy)_2(CO)H]^- + CO_2 \overset{k_{RDS}}{\rightarrow} \rightarrow cis\text{-}[Os(bpy)_2(CO)H]^0 + CO \quad (13)$$

vs a kinetic parameter that is related to Savéant's adimensional λ function.[20] The results of the simulations are compared to experimental data which were averages of from two to five separate CV experiments. For the first mechanism, the results of simulations with k_{RDS} = 10, 20, 30, and 40 M^{-1} s^{-1} are shown in Figure 4B. A satisfactory fit to the experimental data was achieved with k = 35 M^{-1} s^{-1}.[21] For the second mechanism, Figure 4C, the simulation with k_{RDS} = 400 M^{-2} s^{-1} deviates considerably from the experimental points.

In Figure 5 is shown a plot of i_d/i_{CO_2} as a function of $[CO_2]$. At 96% CO and 4% CO_2 (solid square) CO and CO_2 have approximately the same solubilities in CH_3CN.[22] From the consistency of this point with those where CO_2 was diluted with N_2, it can be concluded that CO neither suppresses nor enhances catalytic activity.

The electrochemical data in dry CH_3CN are consistent with a rate law in which CO_2 is reduced by a RDS which is first order in *cis*-$[Os(bpy)_2(CO)H]^-$ and first order in CO_2. In order to account for the products (carbon monoxide and *cis*-$[Os(bpy)_2(CO)H]^0$) and complete the catalytic cycle, a second electron must be added past this point and O^{2-} ion lost from CO_2 as it is reduced. Two plausible reaction sequences are shown in eqs 14–17. In these mechanisms it is assumed that (1) the reaction

$$cis\text{-}[Os(bpy)_2(CO)H]^- + CO_2 \overset{k_1}{\rightarrow} I_a \quad (14)$$

$$2I_a \overset{k_2}{\rightarrow} 2\ cis\text{-}[Os(bpy)_2(CO)H]^0 + CO + CO_3^{2-} \quad (15)$$

$$I_a + CO_2 \overset{k_3}{\rightarrow} cis\text{-}[Os(bpy)_2(CO)H]^+ + CO + CO_3^{2-} \quad (16)$$

$$cis\text{-}[Os(bpy)_2(CO)H]^+ + cis\text{-}[Os(bpy)_2(CO)H]^- \overset{k_4}{\rightarrow} 2\ cis\text{-}[Os(bpy)_2(CO)H]^0 \quad (17)$$

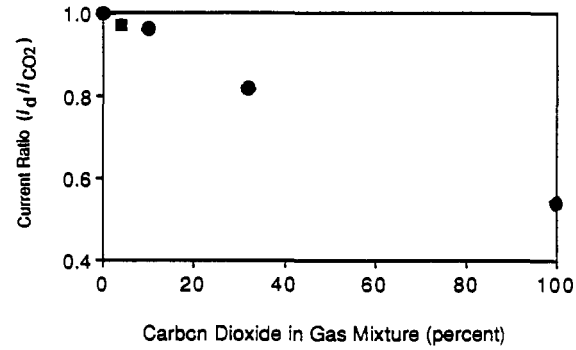

Figure 5. Plot of the current ratio (i_d/i_{CO_2}), as in Figure 4 vs the % CO_2 in CO_2/CO or CO_2/N_2 gas mixtures. Circles: Experiments 2, 6, and 10 from Table III. Box: Average of three CV experiments using a 4% CO_2 and 96% CO gas mixture with *cis*-$[Os(bpy)_2(CO)H][PF_6]$ at 5.0 mM.

between *cis*-$[Os(bpy)_2(CO)H]^-$ and CO_2 gives an intermediate which undergoes electron transfer with a second intermediate with the lost O^{2-} appearing as CO_3^{2-} (eq 15) or (2) O^{2-} loss to CO_2 triggers an intramolecular two-electron transfer (eq 16) with *cis*-$[Os(bpy)_2(CO)H]^+$ appearing in a following comproportionation step, eq 17. At high $[CO_2]$ and low [*cis*-$[Os(bpy)_2(CO)H]^0$], eq 15 could become rate determining in the first case. Computer simulations reveal that if $k_2 > 10^6$ M^{-1} s^{-1}, the self-reaction in equation 15 would be sufficiently rapid that it would not interfere and $k_{obs} = k_1$. At $k_2 = 10^4$ M^{-1} s^{-1}, an increase of 0.1 in the current ratio, i_d/i_{CO_2}, is predicted for $[CO_2]$ = 0.14 M, v = 0.2 V/s, and k_1 = 45 M^{-1} s^{-1} when *cis*-$[Os(bpy)_2(CO)H][PF_6]$ isdecreased from 4.5 to 1.2 mM. A small increase in the current ratio was observed experimentally under these conditions; compare experiments 1 with 25, 2 with 26, and 3 with 27 in Table III.[23]

Constant Potential Electrolysis. Labeling Experiments. As a further test of mechanism, two different isotopic labeling experiments were conducted. When the deuterium labeled complex, *cis*-$[Os(bpy)_2(CO)D][PF_6]$, was used as a catalyst under conditions where formate anion was a significant product, (Table I, experiment 3, >0.2 M H_2O, 20% formate), there was no proton incorporation into the osmium catalyst after 1.8 turnovers with respect to formate anion production. This was shown by monitoring ν(Os–H) in the infrared at 2005 cm^{-1} (see Figure 6A). In the inverse experiment (Table I, experiment 11), 325 μL of D_2O was added to 26 mL of an electrolysis solution making $[D_2O] \approx 0.7$ M. Upon electrolysis to 100 C passed, no decrease in the hydride stretch at 2005 cm^{-1} was observed (see Figure 6B). When $^{13}CO_2$ was used as the source of CO_2, there was no incorporation of ^{13}C into the CO group of the catalyst after 5.5 turnovers of the catalyst with respect to CO formation as shown by IR measurements in the ν(CO) region (Table I, experiment 9; 39 mg of *cis*-$[Os(bpy)_2(CO)H][PF_6]$.[24]

Kinetics: Added Water. The effect of added H_2O was studied by CV at glassy-carbon and Pt electrodes (v = 0.2 V/s; *cis*-$[Os(bpy)_2(CO)H]^+$ = 3.8 mM). At the glassy carbon electrode, there was an initial decrease in the current ratio, i_d/i_{CO_2} as the water concentration was increased, followed by a leveling off as $[H_2O]$ approached 300 mM (Table IV). At a Pt electrode under identical conditions, the current ratio, i_d/i_{CO_2}, showed a similar dependence on $[H_2O]$ with a slightly larger decrease in i_d/i_{CO_2}, presumably due to hydrogen evolution.

(20) (a) Savéant, J.-M.; Vianello, E. *Electrochim. Acta* **1963**, *8*, 905. (b) Amatore, C.; Savéant, J.-M. *Electroanal. Chem. Interfacial Electrochem.* **1983**, *144*, 59 and references therein. (c) The function used was the log $[RT/Fv]$ multiplied by the log $[CO_2]$ or log $[CO_2]^2$ depending on the order in CO_2 where R is the gas constant, T is temperature, F is the Faraday constant, and v is the scan rate. Our function is related to Savéant's adimensional I function by $1/k_{RDS}$ where $I = k_{RDS}[RT/Fv][CO_2]$ or $\lambda = k_{RDS}[RT/Fv][CO_2]2$ depending on the order in CO_2.

(21) Error bars of 5% are shown for the experimental data in Figure 4B.

(22) The solubility of CO_2 is approximately 24 times greater than CO in a variety of solvents with dipole moments in the range (1.7–4.2 D) of that for acetonitrile (3.92 D). See: *Solubilities of Inorganic and Organic Compounds*; Stephen, H., Stephen, T., Eds.; Macmillan Co.: New York, 1963; pp 1053 and 1071.

(23) The predicted increase in the current ratio is based on computer simulations at the highest levels of CO_2 in Table III. At lower CO_2 levels, it is much harder to detect experimentally. The background current is a larger fraction of the overall current, and the predicted current increment is difficult to observe.

(24) By comparison, $^{13}CO_2$ electrolysis experiments in the presence of *cis*-$[Ru(bpy)_2(CO)H][PF_6]$ resulted in the formation of significant amounts of $[Ru(bpy)_2(CO)(NCCH_3)]^{2+}$ and $[Ru(bpy)_2(CO)(OC(O)H)]^{2+}$ (see ref 12).

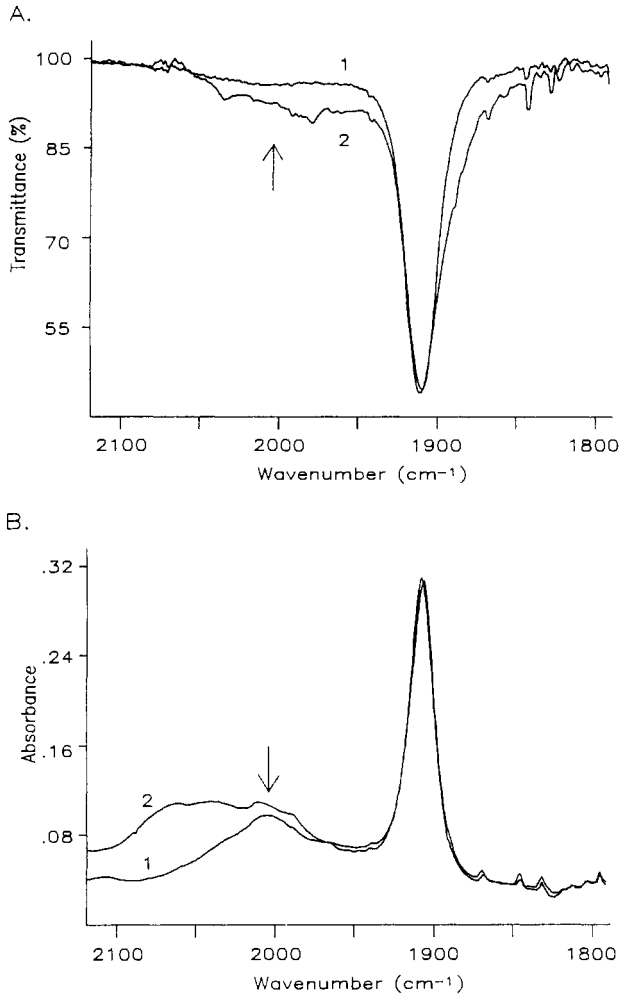

Figure 6. Infrared spectra acquired during constant potential electrolysis. (A) Before (1) and after (2) electrolysis of *cis*-$[Os(bpy)_2(CO)D][PF_6]$, to 40 C, Table I, experiment 3. The arrow at 2005 cm^{-1} shows where ν(Os–H) is observed in *cis*-$[Os(bpy)_2(CO)H][PF_6]$. (B) As in part A but for *cis*-$[Os(bpy)_2(CO)H][PF_6]$ + D_2O (325 μL) to 100 C, Table I, experiment 11. The arrow indicates 2005 cm^{-1}. The original FT-IR spectra were digitized by using un-Plot-It (Silk Scientific) and plotted from Spectra Calc (Galactic Industries).

Table IV. Kinetic Parameters for the Reduction of CO_2 by *cis*-$[Os^{II}(bpy)_2(CO)H]^+$ (3.8 ± 0.1 mM) in 0.1 M TBAH in MeCN in the Presence of H_2O

	current ratio $(i_d/i_{CO_2})^a$		
$[H_2O]$ (mM)	$[CO_2]$ = 45 mM	$[CO_2]$ = 91 mM	$[CO_2]$ = 140 mM
0	0.854	0.741	0.650
27	0.833	0.714	0.631
54	0.820	0.687	0.608
81	0.807	0.671	0.599
108	0.808	0.656	0.584
135	0.798	0.647	0.571
162	0.797	0.639	0.571
189	0.784	0.636	0.560
216	0.781	0.627	0.556
243	0.764	0.623	0.554
270	0.755	0.624	0.556
297	0.755	0.618	0.557

[a] As in Table II at a scan rate of 0.2 V/s at a glassy carbon electrode.

A variety of possible mechanistic cases were considered with added water with the reactions in eqs 9–17 included in the analysis. The dependence of (i_d/i_{CO_2}) on $[H_2O]$ was most satisfactorily fit by a mechanism involving reduction (eqs 9 and 10), followed by a second-order reaction between *cis*-$[Os(bpy)_2(CO)H]^-$ and CO_2 to give I_a, eq 14, followed by a competition for I_a between the

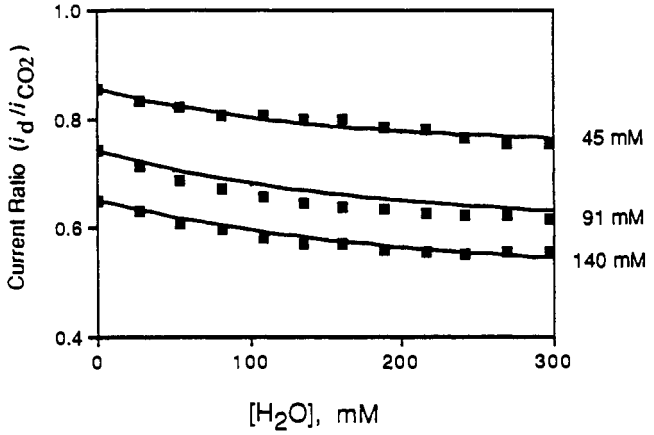

Figure 7. Plot of i_d/i_{CO_2} vs $[H_2O]$ with CO_2 = 45, 91, and 140 mM as indicated. The simulations (—) were based on eqs 9, 10, 14, 15, 18, and 20 with k_1 = 37 M^{-1} s^{-1}, k_2 = 1 × 10^6 M^{-1} s^{-1}, k_5 = 5 × 10^2 M^{-1} s^{-1}, k_7 = 1 × 10^5 M^{-1} s^{-1}, $[CO_2]$ = 45, 91, and 140 mM, and scan rate = 200 mV s^{-1}. Experimental points were taken from Table IV.

self-reaction in eq 15 and a reaction with H_2O. A possible sequence for the H_2O-dependent branch is shown in eqs 18–20. The experimental variation of (i_d/i_{CO_2}) with $[H_2O]$ at a glassy carbon electrode is shown in Figure 7 (boxes).

$$I_a + H_2O \xrightarrow{k_5} I_b + OH^- \quad (18)$$

$$OH^- + CO_2 \xrightarrow{\text{rapid}} HCO_3^- \quad (19)$$

$$I_b \xrightarrow{k_6} cis\text{-}[Os(bpy)_2(CO)H]^+ + HC(O)O^- \quad (20)$$

The conditions for the CV and constant potential electrolysis experiments overlap. In the absence of H_2O, CO is the dominant product. At high concentration of added water, both CO and formate anion are major products of the reaction, but the ratio levels off above $[H_2O]$ = 400 mM. The catalytic current increases with $[H_2O]$ but the effect levels off at $[H_2O] \approx 300$ mM. By inference, CO is the product of the water-independent branch. From the kinetics and the leveling off in the amount of formate anion produced at high $[H_2O]$, the water-dependent branch must lead to both CO and formate. A reaction that would explain the appearance of CO as a product of the H_2O-dependent branch is shown in eq 21. A catalytic cycle which incorporates all of the proposed steps is shown in Scheme I.

$$I_b + CO_2 \xrightarrow{k_7} cis\text{-}[Os(bpy)_2(CO)H]^+ + CO + HCO_3^- \quad (21)$$

Kinetics: CO_2 Reduction by Related Complexes. The kinetics of reduction of CO_2 by a series of related complexes were studied by CV in dry CH_3CN solution (Table V). In all cases current increases occurred in the presence of CO_2 but only upon reduction at the second bpy wave. The complexes studied were *cis*-$[M(bpy)_2(CO)R]^+$ (M = Os, R = Me, Ph; M = Ru, R = CH_2Ph), and *trans*-$[Os(bpy)_2(CO)R]^+$ (R = Me, Et, Ph). As reported in a parallel study, the reduction of CO_2 catalyzed by *cis*-$[Ru(bpy)_2(CO)H]^+$ occurs by a different mechanism involving insertion into the Ru–H bond after the addition of *one* electron.[12]

Values of k_1 (Scheme I) in dry 0.1 M TBAH in CH_3CN solution were estimated by assuming that the mechanism established for *cis*-$[Os(bpy)_2(CO)H][PF_6]$ held throughout the series. Evaluation of k_1 from measurements of i_d/i_{CO_2} was based on the simulations approach. The rate constants are listed in Table V. For the cis complexes, a plot of ln k_1 versus the cone angle of the

Scheme I

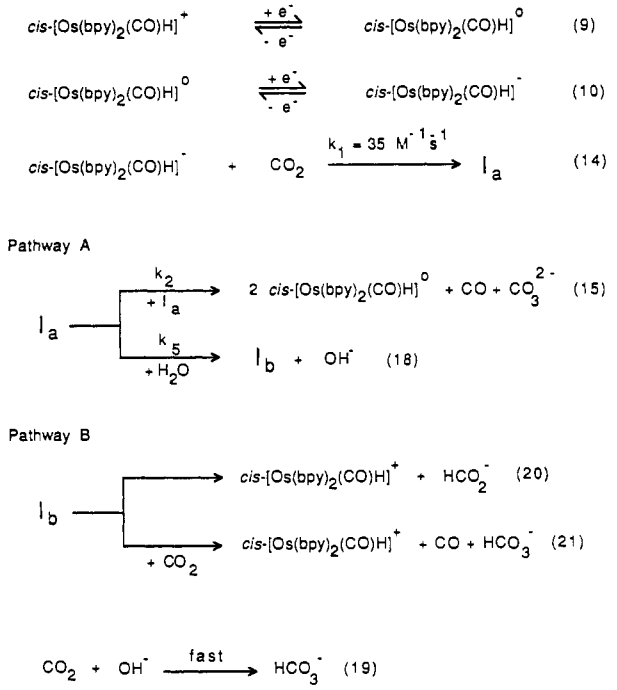

ligand cis to CO (as defined by Tolman[25]) is shown in Figure 8. Several features emerge from these data: (1) there is a linear relationship between ln k, and the molecular volume of the cis ligands as measured by the cone angle, (2) the stereochemically more crowded cis isomers are more sensitive to steric effects than are the trans isomers and when twice-reduced are intrinsically more reactive toward CO_2 (e.g., compare *cis*- and *trans*-$[Os(bpy)_2(CO)Me][PF_6]$ in Table V), and (3) if isomeric intermediates exist for the cis and trans complexes, they are stereochemically rigid under the conditions that lead to CO_2 reduction since from the CV experiments there is no interconversion between isomers.

Discussion. The experiments described here establish that the complex *cis*-$[Os(bpy)_2(CO)H]^+$ is a relatively stable, facile electrocatalyst for the reduction of CO_2 to either CO or formate with oxalate forming at <1%.[26] The reduction is initiated following an initial two-electron reduction of the complex. The catalyst remains intact through a number of redox cycles under conditions where CO or formate are the ultimate products. The appearance of formate anion in the product distribution is favored by added H_2O, and there is an element of product selectivity in the catalysis based on water content.

The most important result of our work is the mechanistic insight that has been gained by kinetic and isotopic labeling studies into how CO_2 is reduced by *cis*-$[Os(bpy)_2(CO)H]^-$. The most powerful insight into mechanism has come from the kinetic study based on the simulation of peak current ratios in cyclic voltammograms. Although this approach is less intuitive than, for example, the pseudo-first-order treatment of peak currents by Nicholson and Shain,[27] it is a more general procedure. As shown by the various fits to possible mechanisms, this approach has the ability to discriminate among mechanistic possibilities if sufficient data are collected as a function of sweep rate and concentration.

In dry CH_3CN, the rate law is first order in CO_2 and in *cis*-$[Os(bpy)_2(CO)H]^-$ (eq 14). At low concentrations of complex, an additional mechanistic feature appears in the data apparently arising from the bimolecular self-reaction of an intermediate (I_a) formed between *cis*-$[Os(bpy)_2(CO)H]^-$ and CO_2 (eq 15). This feature could be successfully incorporated in the simulations. Under our conditions, its contribution to the peak current ratio (i_d/i_{CO_2}) may never exceed 10–20% of the total.

With water added at low levels, a new pathway appears. Its effect on the kinetics was most satisfactorily reproduced by assuming that a competition exists between capture of I_a by a second I_a and capture by added H_2O. As predicted by this mechanism (1) at high concentrations of added water ($[H_2O] \approx 0.3$ M) or at low concentrations of complex the H_2O-dependent pathway increases in importance, (2) the self-reaction of I_a is no longer competitive, and (3) the rate-determining step becomes cleanly the reaction between *cis*-$[Os(bpy)_2(CO)H]^-$ and CO_2.

The results of the controlled-potential electrolysis experiments as a function of added $[H_2O]$ gave further insight into mechanism. With added water, the HCO_2^-/CO product ratio increased, whereas in dry CH_3CN, the product is CO. From the leveling off in peak current and in formate anion as a product with added H_2O, it can be inferred that by $[H_2O] \approx 0.3$ M, I_a channels through the H_2O-based pathway almost completely. Under these conditions *both* HCO_2^- and CO are products of the reduction of CO_2.

All of the available experimental facts have been incorporated into the sequence of reactions in Scheme I. In this scheme (1) there is direct evidence for the k_1 step, from the kinetics, (2) there is at least inferential evidence for the k_2 and k_5 steps, and (3) there is a requirement for separate decomposition pathways for I_b in order to explain CO and HCO_2^- as products from pathway B. The rate constant, k_1, for eq 14, $k = 35 \pm 5$ M^{-1} s^{-1}, is well-defined, but the others in Scheme I are only estimates.[28]

The results of the isotopic labeling and other extrakinetic experiments provide further insight into what occurs mechanistically past the rate-determining step(s). In particular, they provide a basis for considering the microscopic details of the two pathways through which I_a partitions once it is formed. On the basis of the labeling studies, it can be concluded that neither the –CO nor –H groups that were originally bound are directly involved in the mechanism by which CO_2 is reduced although the participation of nonequivalent –CO or –H formed during a catalytic cycle cannot be ruled out.[29] These observations rule out such mechanistic alternatives as initial insertion of CO_2 into the Os–H bond. They also show that the initially bound CO and the CO produced by reduction of CO_2 cannot have occupied equivalent coordination sites in any intermediate that ultimately leads to CO. The CO that is produced in the reduction comes from CO_2. An additional experimental fact that must be accommodated by any reasonable mechanism is the absence of a CO dependence in the rate law.

Intermediate I_a. Even given the limitations imposed by the labeling and kinetic results, there are at least four reasonable formulations for intermediate I_a. They cannot be distinguished by our data. They are as follows: (1) an acyl intermediate, $[Os(bpy)_2(C(O)H)CO_2]^-$, in which the addition of CO_2 induces acyl formation, (2) a higher coordinate, CO_2 addition product, $[Os(bpy)_2(CO_2)(CO)H]^-$, (3) a bpy ring-opened intermediate, $Os(py\text{-}py)(bpy)(CO_2)(CO)H]^-$ where py-py is a monodentate bpy ligand, and (4) a CO_2 adduct of a reduced bpy ligand.[29]

Polypyridyl complexes of Ru and Os are normally stable toward loss of the polypyridyl ligands. In the reduced complexes, metal-based oxidation state isomers such as $[Os^I(bpy)(bpy^-)(CO)H]^-$ or $[Os^0(bpy)_2(CO)H]^-$ could exist as dominant or minority isomers

(25) Tolman, C. A. *Chem. Rev.* **1977**, *77*, 313.
(26) (a) The formation of oxalate anion has been confirmed by ion chromatography but at levels below 1%. (b) Cosnier, S.; Deronsier, A.; Moulet, J. G. *J. Electroanal. Chem. Interfacial Electrochem.* **1986**, *297*, 315. (c) O'Toole, T. N.; Sullivan, B.; Patrick; Bruce, M. R. M.; Margerum, L. D.; Murray, R. W.; Meyer, T. J. *J. Electroanal. Chem. Interfacial Electrochem.* **1989**, *259*, 217.
(27) Nicholson, R. S.; Shain, I. *Anal. Chem.* **1964**, *36*, 706.
(28) Computer simulations based on the assumption that all steps leading up to and including pathway A in Scheme I are operative yield the estimated values: $k_2 \approx 10^4$–10^6 M^{-1} s^{-1} and $k_5 \approx 5 \times 10^2$ M^{-1} s^{-1}.
(29) This possibility was pointed out by the reviewers as was the possible addition of CO_2 to a reduced bpy ligand.

Table V. Cyclic Voltammetric Data in CH_3CN containing 0.1 M TBAH

complex[a]	$E_{1/2}$(Red)[b] (V)	scan rate[c] (mV/s)	current ratio[d] (i_d/i_{CO_2})	k_{est}[e] (M^{-1} s^{-1})	cone angle of L in lig[f]
cis-$[Os^{II}(bpy)_2(CO)H]^+$	−1.34, −1.59	*f*	*f*	35	75
cis-$[Os^{II}(bpy)_2(CO)Me]^+$	−1.37, −1.62	100	0.68	17.5	90
		200	0.80		
cis-$[Ru^{II}(bpy)_2(CO)CH_2Ph]^+$	−1.43, −1.68	100	0.82	7.5	104
		200	0.90		
cis-$[Os^{II}(bpy)_2(CO)Ph]^+$	−1.43, −1.68	100	0.84	6	105
		200	0.91		
trans-$[Os^{II}(bpy)_2(CO)Me]^+$	−1.38, −1.62	100	0.85	≈7	90
		200	0.88		
trans-$[Os^{II}(bpy)_2(CO)Et]^+$	−1.38, −1.61	100	0.88	≈6	102
		200	0.89		
trans-$[Os^{II}(bpy)_2(CO)Ph]^+$	−1.35, −1.58	100	0.89	≈4	105

[a] As PF_6^- salts. [b] Pt working electrode. [c] Cyclic voltammetric data at the scan rate indicated. [d] Ratio of the peak current at the second reduction wave under an inert argon atmosphere to the peak current in the presence of CO_2, $[CO_2]$ = 140 mM. [e] Estimated rate constant by simulation; see text. [f] See ref 25.

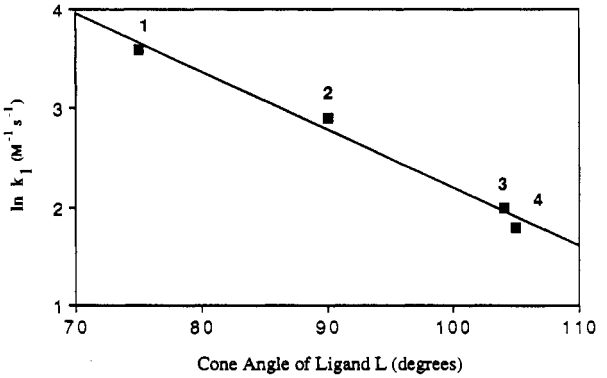

Figure 8. Plot of ln k_1 vs the cone angle of the ligand cis to CO for *cis*-$[Os(bpy)_2(CO)H]^+$ (1), *cis*-$[Os(bpy)_2(CO)Me]^+$ (2), *cis*-$[Ru(bpy)_2(CO)CH_2Ph]^+$ (3), and *cis*-$[Os(bpy)_2(CO)Ph]^+$ (4) with a best-fit straight line drawn to illustrate the nearly linear relationship between them.

in which the added electrons occupy metal-based $d\sigma^*$ levels rather than π^*-based bpy levels. Given the propensity toward five-coordination for electronic configuration d^8, this could initiate ligand loss and open a chelate ring (eq 22).

$$cis\text{-}[Os(bpy)_2(CO)H]^- + CO_2 \rightarrow cis\text{-}[Os(bpy)(py\text{-}py)(CO)(H)CO_2]^- \quad (22)$$

There is precedence for oxidatively-induced coordination sphere expansion, eq 23, in the report of reversible protonation of *trans*-$[Os(bpy)(PPh_3)_2(CO)(H)]^+$ (eq 24).[30] In this reaction, the protonation of Os^{II} can be viewed, at least in a formal sense, as involving a formal oxidation of $(d\pi)^6$ Os(II) to $(d\pi)^4$ seven-coordinate Os(IV).

$$cis\text{-}[Os(bpy)_2(CO)H]^- + CO_2 \rightarrow [Os(bpy)_2(CO)(H)CO_2]^- \quad (23)$$

$$trans\text{-}[Os(bpy)(PPh_3)_2(CO)(H)]^+ + H^+ \rightarrow trans\text{-}[Os(bpy)(PPh_3)(CO)(H)_2]^+ \quad (24)$$

One fact that supports the idea of coordination sphere expansion is the sensitivity of k_1 to the molecular volume of the ligand cis to CO in *cis*-$[M(bpy)_2(CO)R]^+$ = (M = Os, R = H, Me, Ph; M = Ru, R = CH_2Ph), as measured by the Tolman cone angle (Figure 8). There is not, for example, an equivalent sensitivity to the one-electron $E_{1/2}(2)$, or two-electron ($E_{1/2}(1) + E_{1/2}(2)$) potentials of the bpy-reduced complexes as reducing agents. Although the inclusion of the k_1 value for *cis*-$[Ru(bpy)_2(CO)(CH_2Ph)]^-$ in the correlation in Figure 8 may be serendipitous, the relative insensitivity of k_1 to factors other than steric effects is significant. The mechanistic key may lie in the associative addition of CO_2 and the distortions that this addition induces as the ligand environment changes from six- to seven-coordinate. Microscopically, the origin of the steric effect would lie in enhanced force constants and/or restricted amplitudes for those normal modes that are skeletal in nature which are involved in the change in coordination number from 6 to 7. These effects arise from enhanced intra-coordination sphere repulsion as the coordination sphere is expanded. This would lead to an increase in the energy of activation for intramolecular rearrangement as the molecular volume of R increased.

Expansion of the coordination sphere to give pentagonal bipyridyl, capped octahedral, or capped trigonal prismatic intermediates would require participation by an additional, metal-based d orbital.[31] By inference, with CO_2 acting as a Lewis acid, and ultimately as the oxidant, the required change in hybridization at the metal could be accomplished by electron transfer from π^* (bpy) orbitals, acting as electron reservoirs,[32] to an orbital largely $d\sigma^*$ in character to give an orbital set that could accomodate seven coordination.

$$\underset{(d\pi_1)^2(d\pi_2)^2(d\pi_3)^2(\pi_A^*)^1(\pi_B^*)^1}{[(bpy^{\bullet-})_2Os(CO)(H)]^-} + CO_2 \longrightarrow \underset{(d_1)^2(d_2)^2(d_3)^2(d_4)^2}{[(bpy)_2Os(CO)(H)(CO_2)]^-} \quad (25)$$

Although the trans complexes are intrinsically less reactive, their ability to react with CO_2 is revealing. That they act as catalysts shows that there is not a requirement for a cis arrangement for the –CO and –R groups. This is presumably a prerequisite for the formation of formyl (R = H) or acyl intermediates (R = Me, Ph, CH_2Ph). From the absence of trans to cis isomerization under catalytic conditions it can be inferred that a lower coordinate intermediate does not appear as part of the mechanism. Under substitutional conditions, bis-bpy complexes are known to interconvert from trans- to the stereochemically preferred cis-isomer.[33]

If the hint of second-order loss of I_a in the kinetics is correct, eq 15, there is mechanistic precedence. Second-order kinetics have been established by Creutz, Sutin, et al. in the reduction of CO_2 by a cobalt(I) macrocycle.[3h] The intimate details of how these reactions occur are not known. From the second-order

(30) Sullivan, B. P.; Lumpkin, R. S.; Meyer, T. J. *Inorg. Chem.* **1987**, *26*, 1247.

(31) (a) Hoffman, R.; Beier, B. F.; Muetterties, E. L.; Rossi, A. R. *Inorg. Chem.* **1977**, *16*, 511. (b) Drew, M. G. B. *Prog. Inorg. Chem.* **1978**, *23*, 67. (c) Spees, S. T.; Perumareddi, J. R.; Adamson, A. W. *J. Am. Chem. Soc.* **1968**, *90*, 6626.

(32) (a) DeArmond, M. K.; Hillis, J. E. *J. Chem. Phys.* **1971**, *54*, 2247. (b) Sullivan, B. P. *Platinum Met. Rev.* **1989**, *33*, 2. Also see refs 1n, 1u, and 9.

(33) Durham, B.; Wilson, S. R.; Hodgson, D. J.; Meyer, T. J. *J. Am. Chem. Soc.* **1980**, *102*, 600. Also see ref 5b.

nature of the reaction, it can be inferred that of the two electrons required for the reduction to CO one comes from each of the two reduced complexes. As shown in eq 15, the majority pathway results in 2e- reduction at one CO_2 with net transfer of O^{2-} to a second. On the basis of the appearance of oxalate anion as a product of the electrolyses, there may be a competing pathway through eq 15 that results in C–C coupling as well. There are two reports in the literature showing that oxalate is also a product of CO_2 reduction in polymeric films in which known homogeneous catalysts had been incorporated.[26b,c]

Intermediate I_b. The necessity to invoke a second intermediate past the rate-determining step is suggested by the competition between H_2O and the self reaction for I_a. From the appearance of both CO and HCO_2^- as products of the reaction, it can be inferred that capture of I_a by H_2O leads to a second intermediate which can partition in different ways to give either CO or HCO_2^-. The proton source required to give bound formate presumably comes from H_2O (eq 26). One way to explain the competition between CO and HCO_2^- as products is to invoke protonation at either C, to give HCO_2^-, or at O, to give CO. On the basis of the results of the deuterium labeling studies, the appearance of formate cannot involve insertion into the Os–H bond.

$$[(bpy)_2Os(CO)(CO_2)(H)]^- + H_2O \rightarrow [(bpy)_2Os(CO)(HCO_2)(H)]^0 + OH^- \quad (26)$$

$$[(bpy)_2Os(CO)(HCO_2)(H)]^0 \rightarrow [(bpy)_2Os(CO)(H)]^+ + HCO_2^- \quad (27)$$

Acknowledgment. Funding by the Gas Research Institute (Grant 5087-260-1455) and the Office of Naval Research (Grant N00014-87-K-0430) is gratefully acknowledged. Dr. Clifford M. Carlin is thanked for his helpful discussions.

Registry No. *cis*-$[Os(bpy)_2(CO)H]PF_6$, 84117-35-1; *cis*-$[Os(bpy)_2(CO)Me]PF_6$, 143237-17-6; *cis*-$[Ru(bpy)_2(CO)CH_2Ph]PF_6$, 82482-60-8; *cis*-$[Os(bpy)_2(CO)Ph]PF_6$, 143237-18-7; *trans*-$[Os(bpy)_2(CO)Me]PF_6$, 143237-19-8; *trans*-$[Os(bpy)_2(CO)Et]PF_6$, 143237-20-1; *trans*-$[Os(bpy)_2(CO)Ph]PF_6$, 143237-21-2; *cis*-$Os(bpy)_2(CO)H$, 143237-22-3; *cis*-$Os(bpy)_2(CO)Me$, 143237-23-4; *cis*-$Ru(bpy)_2(CO)CH_2Ph$, 143265-79-6; *cis*-$Os(bpy)_2(CO)Ph$, 143237-24-5; *trans*-$Os(bpy)_2(CO)Me$, 143291-66-1; *trans*-$Os(bpy)_2(CO)Et$, 143237-25-6; *trans*-$Os(bpy)_2(CO)Ph$, 143291-67-2; *cis*-$[Os(bpy)_2(CO)H]^-$, 111437-23-1; *cis*-$[Os(bpy)_2(CO)Me]^-$, 111437-17-3; *cis*-$[Ru(bpy)_2(CO)CH_2Ph]^-$, 111437-19-5; *cis*-$[Os(bpy)_2(CO)Ph]^-$, 111437-18-4; *trans*-$[Os(bpy)_2(CO)Me]^-$, 143291-68-3; *trans*-$[Os(bpy)_2(CO)Et]^-$, 143237-26-7; *trans*-$[Os(bpy)_2(CO)Ph]^-$, 143291-69-4; *cis*-$[Os(bpy)_2(CO)H]^+$, 84117-34-0; CO_2, 124-38-9; C, 7440-44-0; Pt, 7440-06-4; CO, 630-08-0; $HC(O)O^-$, 71-47-6; CH_3CN, 75-05-8; TBAH, 3109-63-5; ^{13}C, 14762-74-4; D_2, 7782-39-0; *cis*-$[Os(bpy)_2(CO)(MeCN)]^{2+}$, 89689-75-8; *cis*-$[Os(bpy)_2(MeCN)_2]^{2+}$, 116946-87-3.